JOURNAL OF GEOPHYSICAL RESEARCH, VOL. 95, NO. B11, PAGES 17,661–17,675, OCTOBER 10, 1990

Small-Scale Disequilibrium in a Magmatic Inclusion and its More Silicic Host

JON P. DAVIDSON[1]
Department of Geological Sciences, University of Michigan, Ann Arbor

SHANAKA L. DE SILVA
Lunar and Planetary Institute, Houston, Texas

PETER HOLDEN[1] AND ALEX N. HALLIDAY
Department of Geological Sciences, University of Michigan, Ann Arbor

Basaltic andesite inclusions and their host dacite from the Purico-Chascon complex in northern Chile are isotopically distinct. Textural characteristics of the inclusions are typical of those resulting from magma mingling. Serial sectioning across the interface of an inclusion and its host dacite, complemented by microdrill sampling and detailed microprobe work, has enabled us to examine the scale of mixing and chemical (isotopic and trace element) disequilibrium. The results of this work show that (1) the composition of the inclusion is relatively homogeneous; (2) the dacite host is generally higher in $^{87}Sr/^{86}Sr$ and lower in $^{143}Nd/^{144}Nd$ than the enclave, but it is heterogeneous on a small scale, and probably a "hybrid"; (3) the isotopic composition in the marginal zone, apparently on both host and inclusion sides of the weakly chilled interface, actually shows the highest $^{87}Sr/^{86}Sr$ and lowest $^{143}Nd/^{144}Nd$; (4) large plagioclase crystals in the inclusions and host are xenocrystic, with higher $^{87}Sr/^{86}Sr$ than any of the other samples. These observations are reconciled with a model of magma evolution in a crustal magma chamber. In such a scenario the mafic magma is overlain by a cap of rhyolite - a partial melt of the dacitic ignimbrites which now underlie the Purico-Chascon complex. Overturn of such a magma system gives rise to a hybrid dacite containing discrete mafic inclusions.

1. Introduction

Magmatic inclusions more mafic than their host are a common feature of silicic volcanic and plutonic rocks. While some are demonstrably of cumulus origin [*Bacon and Druitt*, 1988; *Tait*, 1988; *de Silva*, 1989*a*], and others are interpreted as 'restite' [*Wyborn and Chappell*, 1986], the inclusions discussed in this paper belong to the most common group: those thought to be the result of magma mingling [*Walker and Skelhorn*, 1966; *Eichelberger*, 1975; *Bacon and Metz*, 1984; *Bacon*, 1986]. The inclusions are typically spheroidal, are vesicular, have 'cauliform' or crenulate chilled margins which are convex towards the more silicic host, and show crystal morphologies (quench textures) consistent with incorporation in a liquid, or at least partially molten state.

In general, studies of such inclusions and their hosts have been directed towards unraveling their petrogenetic evolution using bulk samples [e.g., *Eichelberger*, 1975; *Grove and Donnelly-Nolan*, 1986; *Holden et al.*, 1987] or modeling the dynamics of the interaction of mafic and silicic magmas [e.g., *Sparks and Marshall*, 1986; *Frost and Mahood*, 1987]. The physical and chemical interactions of the host and intrusive magma on a medial to large scale (hand specimen to magma chamber) are now reasonably well understood. Variables that control the style and amount of magma interaction include temperature, latent heat of fusion, composition, water content, and the relative amounts and total volumes of each endmember, as well as the time and length scales of mixing. However, the interaction of mafic and silicic magmas at small length scales (thin section to micron scale) is less well documented and understood. Results of the few detailed experimental [e.g., *Lesher*, 1988] and petrologic studies [*Koyaguchi*, 1986; *Clynne*, 1989] indicate complex chemical and physical interactions which are lost in studies utilizing bulk samples.

Here, we present an investigation of small-scale isotopic, compositional, and mineralogical variation, by using microsampling techniques, across the interface of a basaltic-andesite inclusion and its dacitic host from Cerro Chascon, a Holocene dome in northern Chile (Figure 1). Earlier work on bulk whole rock samples [*Hawkesworth et al.*, 1982] showed that the inclusions and hosts are isotopically distinct. We contend that our observations lend further insight into the nature and time and length scales of mafic-silicic magma interactions.

2. Geological and Geochemical Background

The inclusion discussed in this study, P8815 (Figure 2; from Cerro Chascon), is one of a suite collected from two domes, Cerro Chascon and Cerro Aspero, located in the Purico complex (67°45'W, 22°57'S) in the Central Volcanic Zone of the Andes (Figure 1). The Purico complex is a broad ignimbrite shield with a summit complex of cones and domes (Figure 1*a*). Earliest activity in the region (from 1.3 to 1.0 Ma) produced the ~80 km^3, dacitic Purico ignimbrite member [*de Silva*, 1989*b*]. Following these major ignimbrite eruptions, the andesite to dacite cones and domes of the summit complex formed. Two groups can be defined on the basis of age and chemistry; the post-ignimbrite but glaciated andesitic Purico group (Cerros Purico sensu stricto, Toco,

[1]Now at Department of Earth and Space Sciences, University of California, Los Angeles.

Paper number 90JB00427.
0148-0227/90/90JB-00427 $05.00

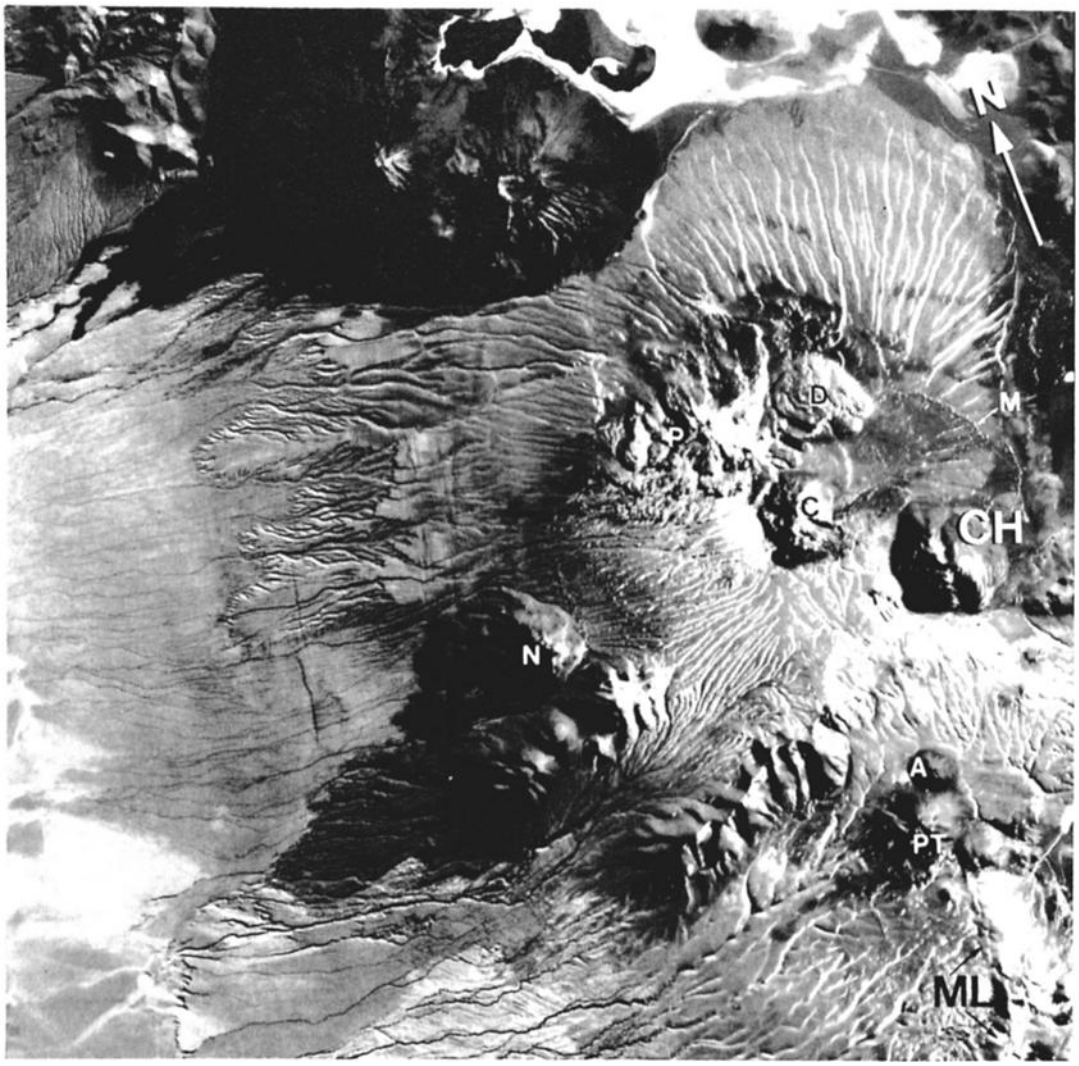

Fig. 1*a*. Landsat Thematic Mapper image of the Purico complex (~45 x 45 km). The complex consists of the Purico ignimbrite member, a large dissected ignimbrite shield (light tone) and endogenous dome (D), on which the younger Purico lava member is built. The latter consists of the Purico group; Cerro Purico sensu stricto (P), Cerro Negro (N), and Cerro Putas (PT); and the Chascon group; Cerro Chascon (CH), Cerro Cerrillo (C), and Cerro Aspero (A). Also shown are the northern extension of the Miscanti lineament (ML) on which Cerros Chascon and Aspero lie and terminal moraines (M) related to the Holocene glaciation (10,000 years B.P.). Image processed and produced at the Lunar and Planetary Institute (Landsat scene 5050614004).

Negro, and Putas, none of which is known to contain inclusions) and the post-glacial (Holocene) dacitic Chascon group (Cerros Cerrillo, Chascon, and Aspero), from which inclusions have been collected. The morphology of the constructs of the two groups also appears to be different; the Purico group are small andesitic polygenetic cones, whereas the Chascon group are dacitic flow-dome complexes; Cerro Aspero could be classified as a Peléan dome. The rocks of the complex are predominantly high-K dacites, with minor volumes of andesite and rhyolite. Domes and lavas range from 56 to 70% SiO_2, while the inclusions analyzed by *Hawkesworth et al.* [1982] are basaltic andesites in the range 52 to 56% SiO_2.

3. Petrography and Mineral Chemistry

The inclusions typically occur as 4 to 25 cm ovoid, subrounded to well-rounded blobs with crenulate margins convex towards the host. Well-preserved chilled margins are often found, and some inclusions show a vesicular core region. In hand specimen, inclusions are aphanitic to microporphyritic in texture, with a rough correlation between groundmass grainsize and size of inclusion. The inclusions compose up to an estimated 20% by volume of some of the Cerro Aspero and Cerro Chascon outcrops. Although *Hawkesworth et al.* [1982] recognized only one type of inclusion (they refer to them as "xenoliths"), *Francis et al.* [1984] recognized two types, which is consistent with our observations. One variety, the "basaltic xenoliths" of *Francis et al.* [1984], has a fine-grained, felty groundmass dominated by skeletal hornblende (resorbed or reacted rims but fresh cores), and plagioclase with subordinate small phenocrysts of olivine and augite. The other variety, the "plutonic xenoliths" of *Francis et al.* [1984], has a fine-grained porphyritic texture but contains no skeletal crystals and does not contain hornblende in the groundmass. Preliminary analyses demonstrate that the olivines and augites in both inclusion types, while different in size, are very similar in

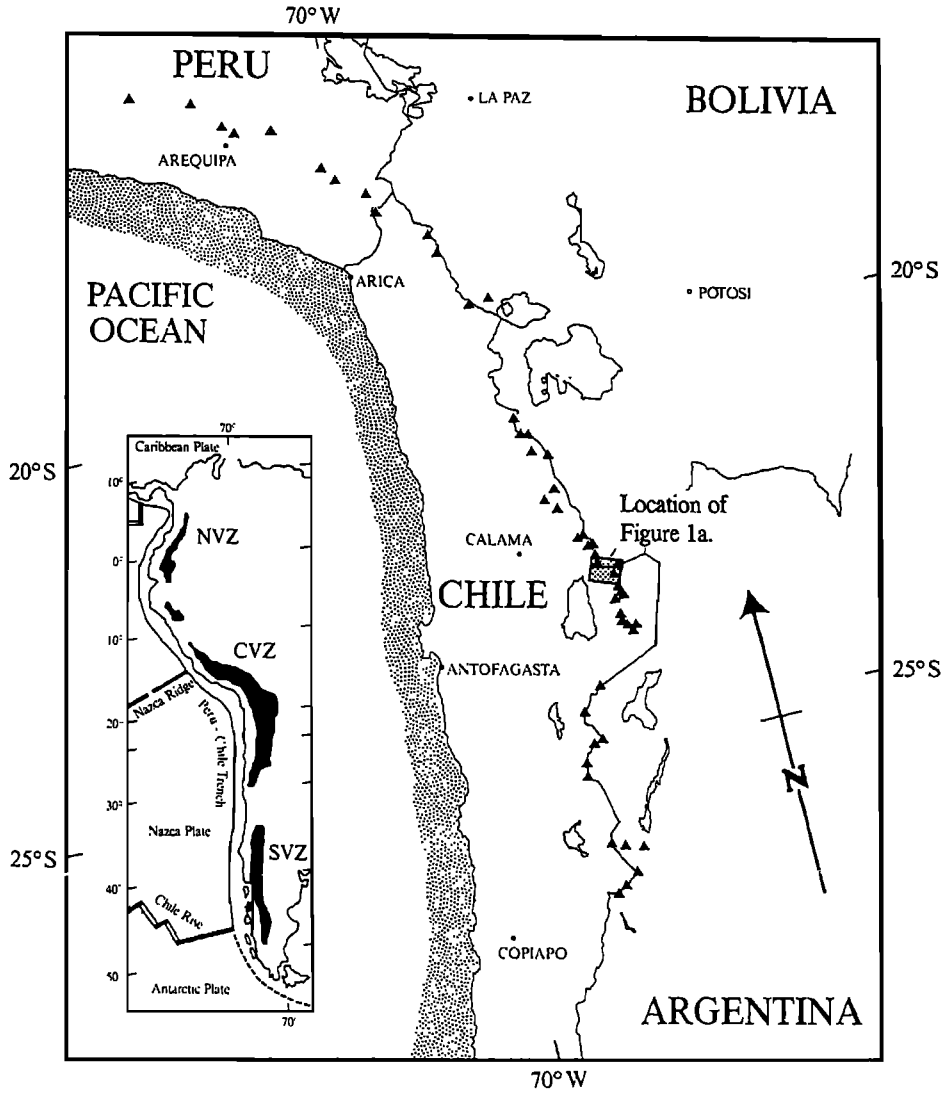

Fig. 1*b*. Map showing the distribution of active volcanoes in the Central Volcanic Zone of the Andes [from *Francis and de Silva*, 1989]. The location of Figure 1*a* is shown.

composition. Inclusion P8815, the subject of this paper, belongs to the second group (i.e., "plutonic xenoliths" of *Francis et al.* [1984]). Representative mineral analyses from this inclusion and its host are given in Table 1.

Basaltic Andesite Inclusion

The inclusion contains crystals of plagioclase, olivine (0.5 - 8 mm) and augite (often in clots) in a microcrystalline groundmass of plagioclase microlites and oxides (Ti-magnetite) up to 0.05 mm with high-Si rhyolite glass. The plagioclases have resorbed, normally zoned cores (Figure 3*a*) ranging from An_{47} to An_{43}, and a rim of An_{63} (Figure 4*a*). Another population is represented by plagioclase phenocrysts which are normally zoned from An_{78} to An_{57}. Groundmass microlites are dominantly An_{72} to An_{65}, but range down to An_{49} (Figure 4*a*). Olivine (Fo_{81-82}) is fresh but shows minor resorption and contains Cr-spinel inclusions. Augite (Mg# 73-82) ranges from $Wo_{45}En_{40}$ to $Wo_{41}En_{44}$ (Figure 4*b*) and has variable Al contents (Table 1). Quartz, hornblende, biotite, and sphene (up to 0.2 mm) are also present and show either textural and/or compositional evidence of being xenocrystic. For instance, quartz is highly resorbed and rimmed with clinopyroxene (Figure 3*b*), while biotites are rimmed with opaques. The core of a large hornblende xenocryst in the analyzed section has a lower Mg# composition very different from those typical of the host and margin (Figure 4*c*).

Selvage

The selvage of the basaltic andesite inclusion is a relatively coarsely crystalline zone with up to 70% crystals dominated by a groundmass of 0.1 - 0.2 mm plagioclase (65%), the majority of which have compositions within the range An_{74} to An_{64} (Figure 4*a*), hornblende (30%), and smaller opaques (5%), defining a hypidiomorphic granular texture set in a matrix of fresh high-Si rhyolite glass (Figure 3*c*). Larger crystals set in this groundmass are olivine, augite, plagioclase, and quartz. The olivines (Fo_{81-82}) are typical of those in the inclusion but are rimmed with augite ($Wo_{45}En_{44}$) and sometimes hornblende (Figure 3*c*). Large plagioclase crystals, up to 0.5 mm, are typically resorbed with normally zoned cores (An_{59} to An_{56}) and more An-rich

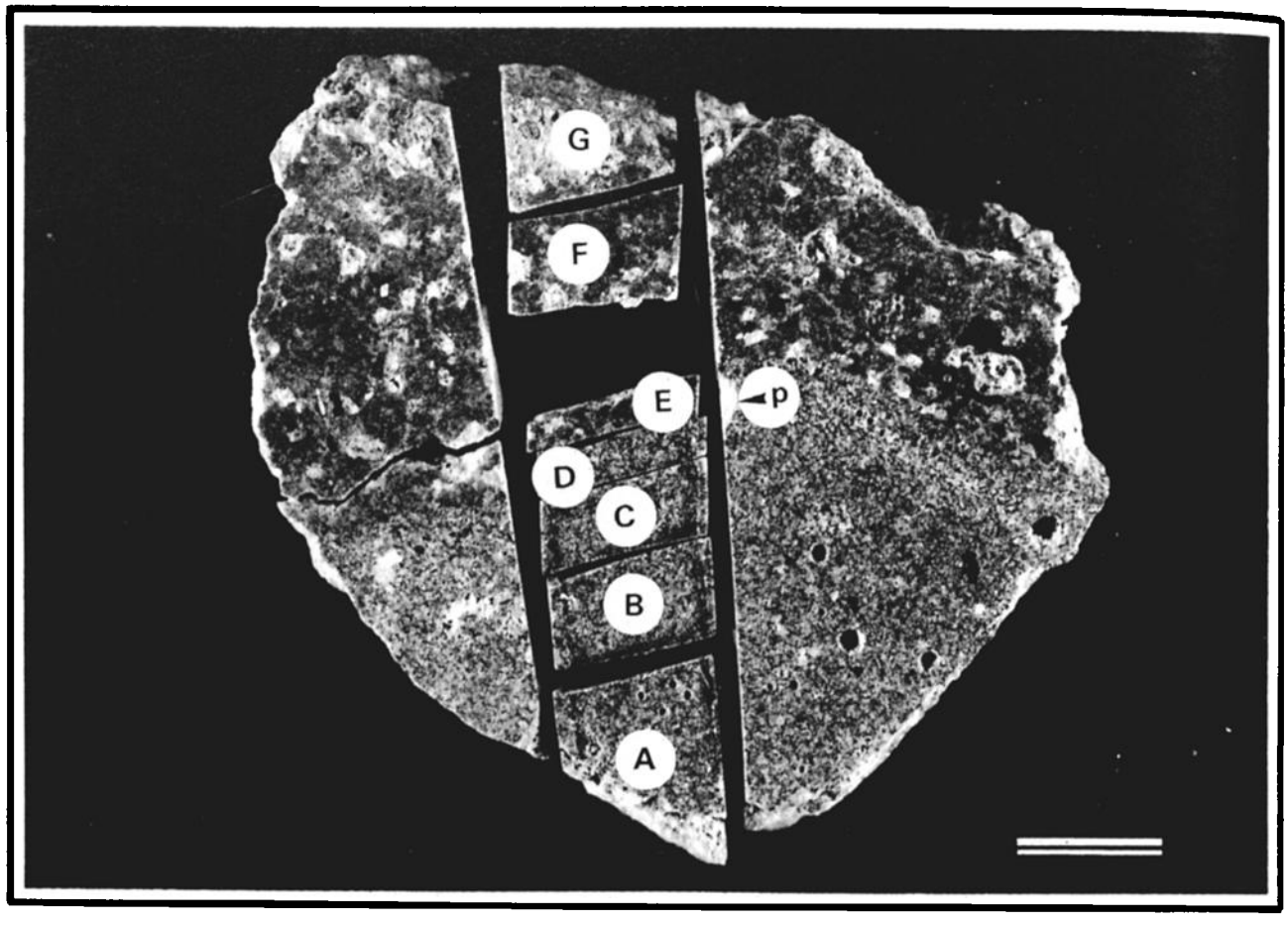

Fig. 2. Photograph of slabbed sample P8815 after slicing samples (chips labeled A through G, shown in Figure 5 and Table 2) in a traverse perpendicular to interface. The contact between the inclusion and host is marked by a narrow reaction zone/chill, referred to in the text as the "selvage". Note the large plagioclase xenocryst (labeled "p" and truncated by slicing subsequent to microdrill sampling (cf. Figure 6*a*) incorporated within the enclave. Scale bar is 1 cm.

rims of An_{73}. The other plagioclases are typically normally zoned and define two groups with compositions ranging from An_{65} to An_{45} and from An_{42} to An_{38} (Figure 4*a*). Resorbed quartz and sphene (titanite) are also present and show signs of disequilibrium, although the quartz has no reaction rim. Rare hornblendes with low Mg# cores are found (Figure 4*c*).

Dacite Host

The host dacite contains phenocrysts of plagioclase with complex zoning, rounded quartz, fresh hornblende and biotite, abundant euhedral sphene (both as inclusions in biotite or discrete microphenocrysts) set in a fine-grained groundmass of plagioclase microlites, opaques, and fresh high-Si rhyolite glass (Figure 3*d*). The plagioclase phenocrysts define two distinct populations; the first are normally zoned (Normal, type N) with compositions in the range An_{78} to An_{67} (core to rim), while the second are reversely zoned (Reverse, type R) over a small range from An_{41} to An_{45}. The plagioclase microlites generally have compositions ranging from An_{41} to An_{49} similar to the type R plagioclases (Figure 4*a*). Hornblende and biotite phenocrysts are unzoned and have restricted compositions. Quartz is sub-rounded. Augites and rare olivines showing resorption or mantling by hornblende are also common. The textural relations and compositions of augite and olivine indicate that they were originally phenocrysts from the inclusion magma, now present as xenocrysts in the more silicic host. Rare low Mg# hornblendes are also found (Figure 4*c*) and are interpreted as xenocrysts from another silicic magma. This mixed crystal population and the presence of small fragments of inclusion indicates that the host dacite is a "hybrid".

Disequilibrium mineral assemblages and textures occur in both inclusion and host, indicating that phenocrysts from both magma types have been exchanged, at least on a local scale. For instance, the association of Mg-rich olivine with quartz, reaction rims on quartz (Figure 3*b*), augite and olivine rimmed by hornblende, and the complex compositional zonations in the plagioclases (see below) are all common indicators of both thermal and chemical disequilibrium [e.g., *Bacon and Metz*, 1984]. Textural evidence suggests that the mafic magma was at (or below) the liquidus, crystallizing olivine, augite and plagioclase prior to being included. Interaction between the two magmas can be examined at a higher resolution by considering the plagioclase compositions in more detail. Two broad populations of plagioclase can be recognized; those with compositions $An_{>60}$ defined by the groundmass plagioclases of both the inclusion and its selvage, and those with $An_{<60}$ typical of groundmass plagioclases (microlites) in the host. These two

TABLE 1*a*. Representative Microprobe Analyses of Minerals: Inclusion

	Plagioclase						Olivine		Augite		Hornblende		Glass
	C	I	R	C	R	Groundmass	1	2	1	4	C	R (augite)	
SiO_2	56.12	57.69	51.09	49.02	55.63	50.64	38.93	38.97	46.83	51.74	44.00	46.99	76.80
TiO_2	0.00	0.01	0.01	0.02	0.02	0.07	0.00	0.01	1.18	0.27	1.47	1.20	0.28
Al_2O_3	27.82	26.78	29.69	31.41	27.78	30.12	0.01	0.11	7.21	2.15	8.68	7.54	13.42
FeO	0.18	0.34	0.41	0.53	0.55	0.98	16.75	16.56	8.70	6.88	16.37	9.49	1.19
MnO	0.00	0.01	0.00	0.01	0.00	0.00	0.31	0.26	0.24	0.22	0.51	0.19	0.05
MgO	0.00	0.43	0.03	0.07	0.12	0.15	42.64	42.68	13.49	16.77	11.51	14.44	0.09
CaO	9.63	8.69	12.46	15.31	11.28	13.88	0.16	0.16	20.28	19.41	11.78	17.07	0.60
Na_2O	5.59	5.67	3.94	2.57	3.78	3.35	0.01	0.00	0.26	0.17	1.31	0.99	1.53
K_2O	0.46	0.85	0.26	0.15	0.91	0.25	0.00	0.00	0.02	0.02	1.05	0.32	2.57
P_2O_5	0.00	0.01	0.02	0.00	0.01	0.03	0.00	0.02	0.03	0.03	0.01	0.00	0.06
SrO	0.11	0.14	0.14	0.17	0.14	0.16	0.23	0.00	0.01	0.00	0.00	0.07	
Cr_2O_3	0.00	0.00	0.02	0.00	0.00	0.01	0.01	0.02	0.12	0.17	0.01	0.02	0.02
Total	99.90	100.24	98.06	99.25	100.22	99.62	98.84	98.69	98.35	97.83	96.70	98.32	96.61
Formula Units per Indicated Number of Oxygens													
	Plagioclase (8 O's)						Olivine (4 O's)		Augite (6 O's)		Hornblende (23 O's)		
	C	I	R	C	R	Groundmass	1	2	1	4	C	R (augite:6 O's)	
Si	2.4008	2.4494	2.3705	2.2337	2.5104	2.3289	0.9420	0.9423	1.6809	1.8370	6.6845	1.7823	
Ti	0.0000	0.0002	0.0005	0.0005	0.0008	0.0024	0.0000	0.0001	0.0317	0.0072	0.1684	0.0342	
Al	1.4027	1.3401	1.6238	1.7519	1.4813	1.6327	0.0003	0.0031	0.3049	0.0898	1.5537	0.3370	
Fe	0.0063	0.0120	0.0159	0.0204	0.0206	0.0377	0.3391	0.3349	0.2612	0.2044	2.0796	0.3010	
Mn	0.0000	0.0003	0.0000	0.0002	0.0000	0.0000	0.0063	0.0053	0.0071	0.0067	0.0654	0.0061	
Mg	0.0000	0.0272	0.0024	0.0045	0.0078	0.0099	1.5382	1.5387	0.7219	0.8876	2.6061	0.8165	
Ca	0.4414	0.3955	0.6195	0.7597	0.5395	0.6842	0.0042	0.0041	0.7801	0.7384	1.9180	0.6939	
Na	0.4635	0.4669	0.3541	0.2286	0.3232	0.2987	0.0002	0.0001	0.0184	0.0114	0.3856	0.0724	
K	0.0249	0.0460	0.0152	0.0089	0.0522	0.0146	0.0000	0.0000	0.0009	0.0008	0.2033	0.0156	
Mg#							81.94	82.13	73.42	82.28	55.61	73.06	
An	47.47	43.53	62.66	76.18	58.97	68.59							
Ab	49.84	51.40	35.81	22.93	35.32	29.95							
Or	2.68	5.07	1.53	0.89	5.70	1.46							

C, core; I, intermediate and R, rim.

TABLE 1*b*. Representative Microprobe Analyses of Minerals: Selvage

	Plagioclase						Augite				Hornblende		Biotite	Sphene	Olivine		Glass
	C	R	C	I	R	Groundmass	C	R	C	R					C	R (augite)	
SiO_2	58.02	57.88	55.73	56.58	49.69	50.67	51.42	51.88	46.92	48.40	41.13	36.10	36.21	28.38	38.86	49.29	77.45
TiO_2	0.01	0.02	0.02	0.05	0.01	0.03	0.26	0.33	1.26	0.72	1.84	3.94	3.94	34.88	0.00	0.48	0.36
Al_2O_3	26.79	26.27	27.90	27.41	31.95	31.40	2.56	2.52	7.15	4.76	13.41	14.08	14.17	1.49	0.01	4.48	12.68
FeO	0.20	0.21	0.55	6.39	0.05	0.60	6.52	6.75	8.40	7.80	12.35	18.54	18.62	1.81	16.86	8.02	1.12
MnO	0.00	0.01	0.00	0.27	0.00	0.00	0.20	0.21	0.19	0.02	0.13	0.28	0.33	0.13	0.31	0.22	0.05
MgO	0.00	0.01	0.12	0.13	0.06	0.06	16.52	16.32	13.48	13.75	13.33	12.78	12.58	0.01	42.52	14.61	0.11
CaO	8.17	7.98	11.18	10.80	14.78	14.55	20.78	20.65	20.71	22.34	11.25	0.00	0.00	25.75	0.16	21.35	0.58
Na_2O	6.28	6.34	3.70	3.71	2.92	2.96	0.16	0.18	0.27	0.22	2.05	0.49	0.47	0.01	0.00	0.22	1.18
K_2O	0.57	0.61	0.91	0.95	0.22	0.26	0.00	0.00	0.01	0.01	0.67	9.60	9.45	0.00	0.00	0.00	3.29
P_2O_5	0.02	0.01	0.01	0.03	0.01	0.04	0.01	0.04	0.03	0.00	0.06	0.02	0.01	0.07	0.01	0.00	0.08
SrO	0.00	0.09	0.14	0.06	0.05		0.00	0.03	0.02	0.05	0.04	0.00	0.01	0.04	0.00	0.00	0.00
Cr_2O_3	0.00	0.00	0.00	0.02	0.00	0.02	0.19	0.17	0.11	0.06	0.02	0.02	0.04	0.00	0.01	0.04	0.00
Total	100.06	99.44	100.27	100.41	100.21	100.60	98.63	99.07	98.53	98.25	96.28	95.85	95.83	92.57	98.74	98.71	96.90

Formula Units per Indicated Number of Oxygens

	Plagioclase (8 O's)						Augite (6 O's)				Hornblende (23 O's)		Bi (22 O's)	Sp (4 O's)	Olivine (4 O's)	
	C	R	C	I	R	Groundmass	C	R	C	R					C	R (augite: 6 O's)
Si	2.5960	2.6084	2.5104	2.4703	2.2740	2.3016	1.9231	1.9317	1.7806	1.8441	6.1627	5.750	5.5139	0.8044	0.9987	1.8601
Ti	0.0002	0.0008	0.0008	0.0016	0.0004	0.0010	0.0073	0.0091	0.0359	0.0205	0.2076	0.472	0.4507	0.7438	0.0000	0.0137
Al	1.4129	1.3952	1.4813	1.4104	1.7232	1.6812	0.1128	0.1104	0.3199	0.2137	2.3678	2.643	2.5433	0.0498	0.0002	0.1994
Fe	0.0075	0.0081	0.0206	0.2333	0.0020	0.0228	0.2039	0.2101	0.2666	0.2484	1.5471	2.469	2.3709	0.0428	0.3624	0.2532
Mn	0.0000	0.0005	0.0000	0.0100	0.0000	0.0000	0.0064	0.0067	0.0060	0.0005	0.0168	0.038	0.0424	0.0032	0.0066	0.0069
Mg	0.0003	0.0006	0.0078	0.0085	0.0038	0.0041	0.9208	0.9058	0.7624	0.7808	2.9772	3.034	2.8559	0.0004	1.6288	0.8217
Ca	0.3918	0.3852	0.5395	0.5052	0.7248	0.7082	0.8328	0.8238	0.8421	0.9121	1.8052	0.000	0.0000	0.7822	0.0045	0.8634
Na	0.5446	0.5540	0.3232	0.3142	0.2588	0.2607	0.0119	0.0127	0.0198	0.0164	0.5947	0.152	0.1379	0.0005	0.0000	0.0164
K	0.0327	0.0351	0.0522	0.0531	0.0127	0.0151	0.0001	0.0000	0.0003	0.0003	0.1283	1.950	1.8352	0.0000	0.0000	0.0000
Mg#							81.87	81.17	74.09	75.86	65.80	55.14	54.64		81.8	76.44
An	40.43	39.53	58.97	57.90	72.76	71.97										
Ab	56.20	56.86	35.32	36.01	25.97	26.50										
Or	3.37	3.61	5.70	6.09	1.27	1.53										

C, core; I, intermediate and R, rim. Selvage as defined in Figure 6.

TABLE 1c. Representative Microprobe Analyses of Minerals: Host

	Plagioclase					Biotite	Hornblende		Augite	Glass
	C	R	C	R	Groundmass					
SiO_2	51.13	48.70	57.44	56.88	55.76	36.71	41.87	43.13	50.19	78.01
TiO_2	0.07	0.02	0.00	0.00	0.02	4.23	2.27	1.39	0.37	0.29
Al_2O_3	30.64	32.41	26.64	27.39	27.02	14.35	12.58	9.39	2.65	12.50
FeO	0.60	0.53	0.18	0.22	0.00	16.03	11.75	16.68	8.02	1.03
MnO	0.00	0.01	0.00	0.00	0.07	0.20	0.14	0.48	0.29	0.02
MgO	0.09	0.07	0.01	0.01	10.08	14.22	14.08	11.28	16.60	0.31
CaO	14.69	15.46	8.31	9.22	7.40	0.01	11.53	11.75	19.40	0.81
Na_2O	1.95	2.57	6.16	5.86	4.78	0.63	1.92	1.37	0.18	1.55
K_2O	0.53	0.15	0.56	0.49	0.54	9.33	0.67	1.18	0.01	2.65
P_2O_5	0.05	0.00	0.01	0.00	0.05	0.00	0.04	0.02	0.01	0.03
SrO	0.11	0.17	0.15	0.10	0.00	0.02	0.07	0.00	0.08	0.00
Cr_2O_3	0.00	0.00	0.00	0.00	0.00	0.02	0.01	0.04	0.02	0.00
Total	99.87	100.07	99.46	100.17	99.07	95.75	96.92	96.71	98.52	97.91
Formula Units per Indicated Number of Oxygens										
	Plagioclase (8 O's)					Bi (22 O's)	Hb (23 O's)		Aug 6 O's)	
	C	R	C	R	Groundmass					
Si	2.3356	2.2337	2.5905	2.5527	2.4757	5.5125	6.2144	6.5810	1.9026	
Ti	0.0023	0.0005	0.0001	0.0000	0.0007	0.4778	0.2530	0.1596	0.0105	
Al	1.6496	1.7519	1.4164	1.4488	1.4141	2.5400	2.2005	1.6864	0.1185	
Fe	0.0230	0.0204	0.0068	0.0082	0.0000	2.0128	1.4580	2.1270	0.2543	
Mn	0.0001	0.0002	0.0000	0.0000	0.0026	0.0258	0.0174	0.0616	0.0093	
Mg	0.0062	0.0045	0.0003	0.0004	0.6672	3.1828	3.1153	2.5643	0.9378	
Ca	0.7189	0.7597	0.4014	0.4436	0.3552	0.0018	1.8334	1.9193	0.7878	
Na	0.1723	0.2286	0.5388	0.5099	0.4115	0.1843	0.5538	0.4050	0.0132	
K	0.0311	0.0089	0.0322	0.0283	0.0306	1.7876	0.1273	0.2291	0.0003	
Mg#						55.62	58.60	60.33	88.78	
An	77.95	76.18	41.28	45.18	44.55					
Ab	18.69	22.93	55.41	51.94	51.61					
Or	3.37	0.89	3.31	2.88	3.84					

C, core; I, intermediate and R, rim.

groups are believed to reflect crystallization from mafic ($An_{>60}$) and silicic ($An_{<60}$) endmembers and on this basis the following interpretations can be made:

1. Microlite compositions in host and inclusion are distinct and reflect crystallization within each respective system (host and inclusion) after they had formed.

2. The cores of the type N and R plagioclases of the host represent phenocrysts which were in equilibrium with mafic and silicic endmember magmas, respectively. The rim compostions reflect re-equilibration with a new "hybrid" melt environment resulting from interaction with the mafic magma. Note that the (hypothetical) mafic and silicic endmember components are not strictly equivalent to the inclusion and host, as some interaction has taken place between them during inclusion formation.

3. The type N plagioclase of the host indicate that phenocrysts crystallizing in the mafic magma were mixed into the silicic magma; which is also borne out by the presence of ubiquitous discrete olivine and augite xenocrysts in the host.

4. The normally zoned resorbed cores of large plagioclases in the inclusion are captured plagioclase phenocrysts from the silicic endmember which were then resorbed and overgrown by a more An-rich rim in equilibrium with the inclusion magma.

A group of xenocrysts foreign to both inclusion and host are present - a few large hornblendes have lower Mg#'s than hornblendes in the present host and margin (Figure 4*c*). This suggests that these xenocrystic hornblendes, and probably some of the quartz and plagioclase, are derived from another (lower temperature) silicic magma, which, as we develop further later, was most likely an ignimbrite precursor to the present dacite host. Most of the crystals in the host are true phenocrysts; i.e., they crystallized from the hybrid dacite, but they crystallized after interaction and mixing with a mafic component (inclusion precursor). This is required because the hornblende crystallized on rims of xenocrystic augite in the host has the same composition as the phenocrysts in the dacite (Figure 4*c*): this would not be the case if the hornblende phenocrysts had been present in the dacite before interaction with the mafic magma.

4. Small-Scale Isotopic Results

Sample P8815 was slabbed (1 cm thick), and a detailed traverse was made (Figure 2) by cutting seven chips over a distance of 5-7 cm perpendicular to the inclusion-host interface (chips labeled A to G in the diagrams). The inclusion, not recovered whole, is estimated to have a diameter of about 5 to 10 cm. The chips were dissolved and analyzed for Sr, Nd, and Pb isotopic composition (Table 2 and Figure 5*a*). Pb isotope variations were not very large, but overall $^{206}Pb/^{204}Pb$ mirrors $^{87}Sr/^{86}Sr$ (Table 2). Although Pb isotopes will form an important part of future work, we will not discuss the Pb data further here. Aliquots were also spiked for determination of Sr, Nd and Pb elemental concentrations (Table 2 and Figure 5*b*).

Before sectioning, eight sites were sampled with a microdrill to determine Sr isotopic variation on the smallest scale (Figure 5*c*). The microdrill sites on sample P8815 and an additional host-inclusion sample, P8823, are illustrated in Figure 6. Some sites comprised multiple drill holes (three to

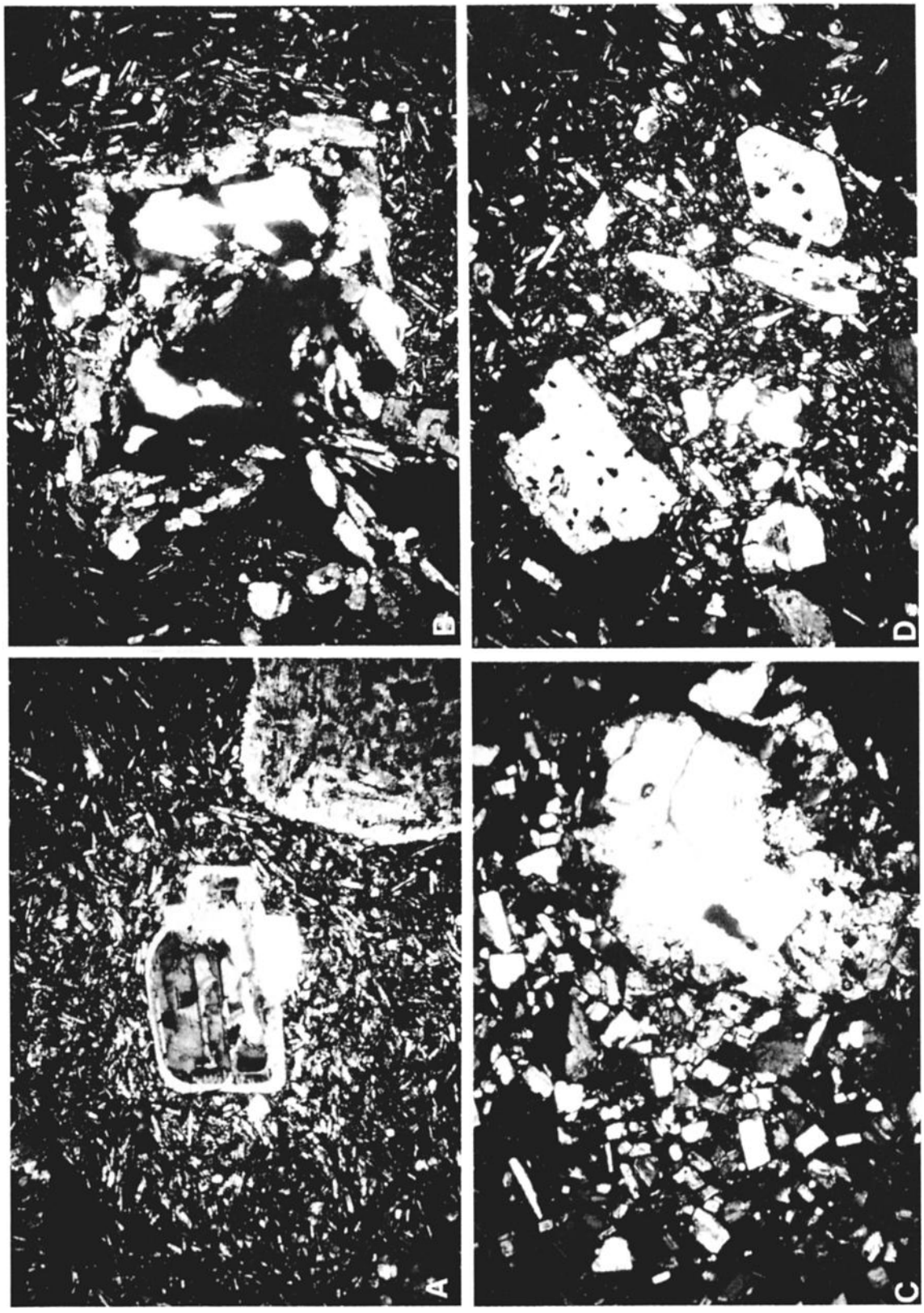

Fig. 3. Photomicrographs showing various features of sample P8815. All views are ~2.7 mm across and were taken under crossed nicols. (*a*) Inclusion: reversely zoned plagioclase xenocrysts set in a highly crystalline groundmass of plagioclase microlites, oxides and glass. Some isolated augites are also present in this view. (*b*) Inclusion: highly resorbed quartz xenocryst rimmed with augite. (*c*) Selvage: large olivine xenocryst rimmed by augite and hornblende in an equigranular groundmass of plagioclase, hornblende, Ti-magnetite, and glass. (*d*) Host: typical view showing phenocrysts of plagioclase, biotite, hornblende, and sphene in a groundmass of plagioclase and fresh glass. Quartz is found but not seen in this view.

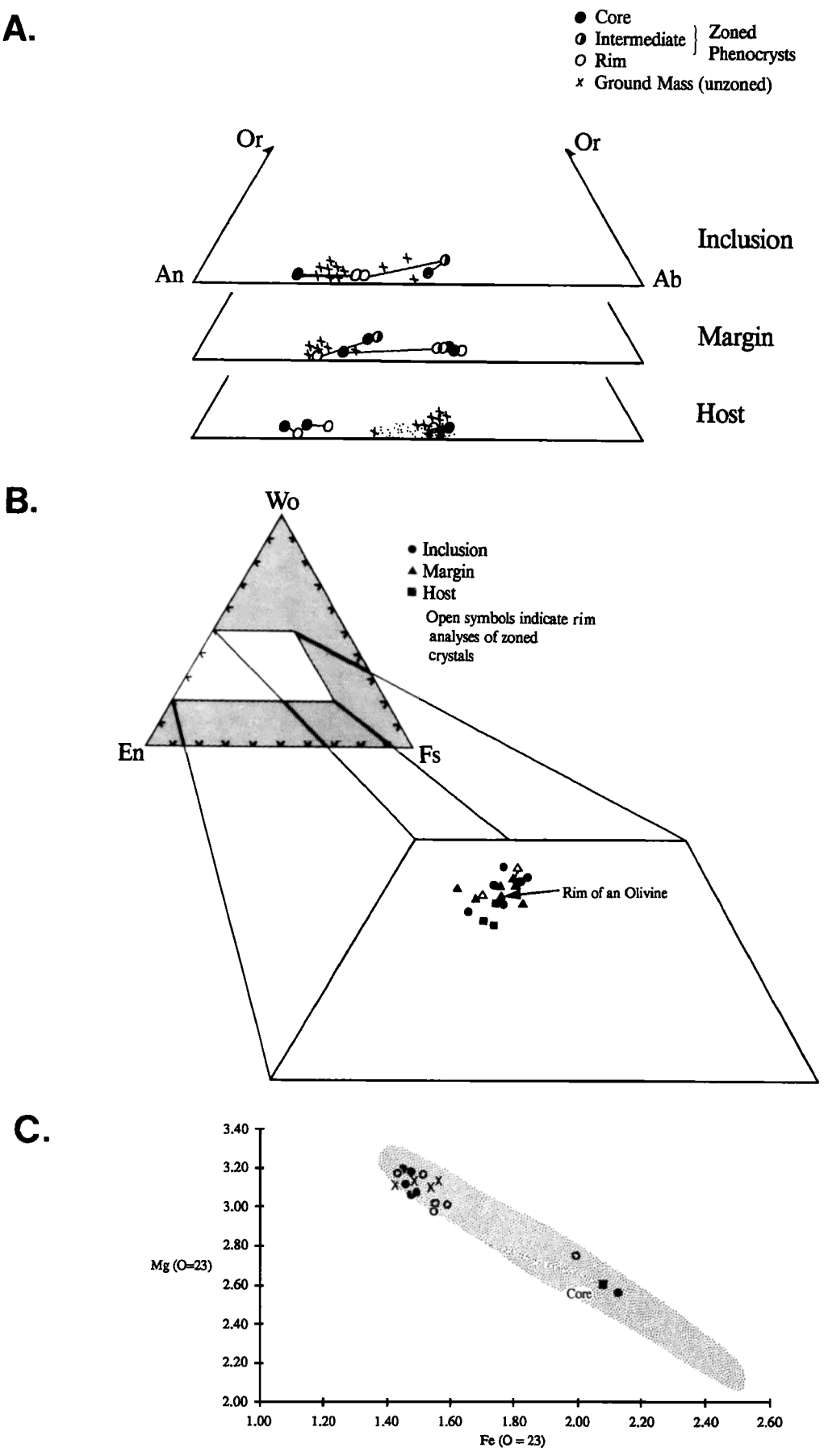

Fig. 4. Variation diagrams comparing mineral chemistry from inclusion, margin and host of sample P8815 (data from Table 1). (*a*) Plagioclase, (*b*) augite compositions, and (*c*) hornblende compositions (inclusion, solid squares; margin, solid circles; host, open circles; and rims to augite xenocrysts in host, crosses.) Stippled fields in Figures 4*a* and 4*c* represent the range of compositions in dacitic ignimbrites in the region (data from *de Silva* [1987]).

TABLE 2. Elemental and Isotopic Compositions of Chips Cut in Traverse (Figure 2)

Section	Sr (ppm)	Nd (ppm)	Pb (ppm)	$^{87}Sr/^{86}Sr$	$^{143}Nd/^{144}Nd$	ε_{Nd}	$^{206}Pb/^{204}Pb$	$^{207}Pb/^{204}Pb$	$^{208}Pb/^{204}Pb$
A	470.7	15.3	8.76	0.706113 ± 15	0.512430 ± 8	-4.1	18.86	15.70	38.91
B	523.8	16.2	9.33	0.706209 ± 14	0.512428 ± 9	-4.1	18.85	15.68	38.86
C	500.2	16.7	9.36	0.706110 ± 12	0.512436 ± 7	-3.9	18.84	15.67	38.16
D	495.0	17.3	9.36	0.706129 ± 16	0.512441 ± 8	-3.8	18.85	15.68	38.84
E	755.1	33.3	14.26	0.706735 ± 13	0.512359 ± 9	-5.4	18.88	15.70	38.97
F	214.5	9.1	14.05	0.706650 ± 13	0.512373 ± 10	-5.2	18.86	15.68	38.89
G	418.1	17.0	13.71	0.706432 ± 15	0.512395 ± 15	-4.7	18.89	15.70	38.96

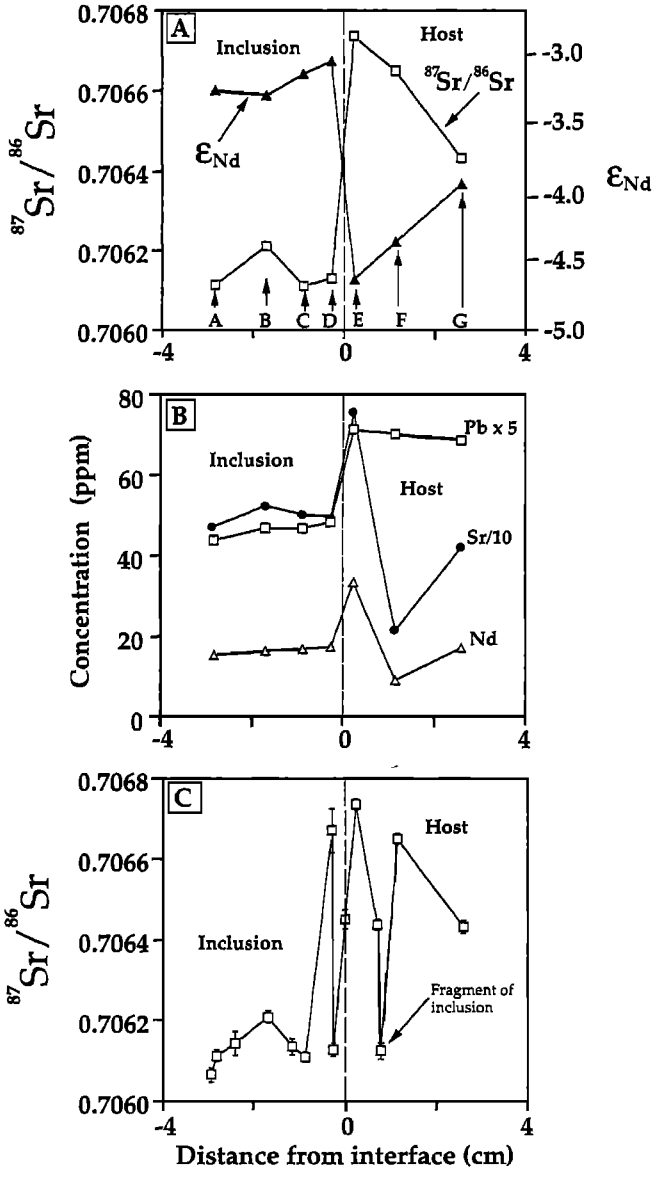

Fig. 5. Results of traverse from inclusion to host (slices as in Figure 2; data in Table 2). (*a*) $^{87}Sr/^{86}Sr$ ratios and ε_{Nd} determined on chips, (*b*) elemental concentrations of Sr, Nd, and Pb determined on chips, and (*c*) $^{87}Sr/^{86}Sr$ results for finest scale (microdrill) sampling (sites shown in Figure 6*a*). Drilling locations are expressed in terms of distance normal to the inclusion-host interface. Some of the drillholes can be seen by close inspection of Figures 2 or 6*a*.

six) but a set of single holes, some of which can be seen on the photographs (Figures 2 and 6), were drilled in the host, inclusion, selvage, and one of the large plagioclase xenocrysts. Mass estimates based on the volume of sample recovered for a drill diameter of 0.5 mm and comparable hole depth suggest that about 1 mg of sample was obtained. The small sample size and the difficulties inherent in determining precise sample weights precluded determination of elemental concentrations through isotope dilution, and caused Sr isotopic ratios to be less precisely measured than would be possible on large samples. Nevertheless, the total range in Sr isotope ratios is far greater than analytical error, and these data can be used to place important constraints on the evolution of the magma system. Analysis of Nd isotopic ratios on the microsamples was largely unsuccessful but should be possible with improvement of mass spectrometric technique.

Isotopic analyses were made on a VG Sector mass spectrometer at the University of Michigan, using a multidynamic (peak-hopping) collection routine. Analysis of the small Sr samples was facilitated by loading in a Ta oxide slurry to improve the Sr signal. A total process Sr blank of 70 pg was measured (amounting to less than 0.02% of the Sr analyzed in the microsamples). The microdrill bit (after total dissolution of the bit) was found to contain 400 pg (Sr) and 130 pg (Nd). However, no significant degradation of the bit was observed after each hole was drilled.

The main points of note from Figures 5 and 6 are as follows:

1. Nd and Sr isotope data on the finest scale (microdrill samples) exhibit more variability in the host than in the inclusion.

2. Trace element concentrations reach a maximum at the inclusion-host interface (chip E; Figure 2). $^{87}Sr/^{86}Sr$ is highest , and $^{143}Nd/^{144}Nd$ lowest, also at the interface, both on the host side (chip E) and, apparently, on the inclusion side of the weak chill (see the set of three microdrill sites in the selvage analyzed at $^{87}Sr/^{86}Sr$ = 0.706671 ± 54 Figure 6*a*).

3. The presence of small chilled fragments of inclusion within the host with disequilibrated isotopic compositions (Figure 5*c*) suggests that solid-state chemical and tracer diffusion was insignificant.

The microdrilled samples from the cores of the largest (>2 mm) plagioclase crystals in both inclusions and host (for two samples: P8815 and P8823 (Figure 6)) are characterized by consistently higher $^{87}Sr/^{86}Sr$ ratios (>0.708). This cannot be reconciled with crystallization from the host dacite ($^{87}Sr/^{86}Sr \approx 0.7068$) and suggests that these large crystals were originally phenocrysts from a magma with a greater crustal Sr component, and are

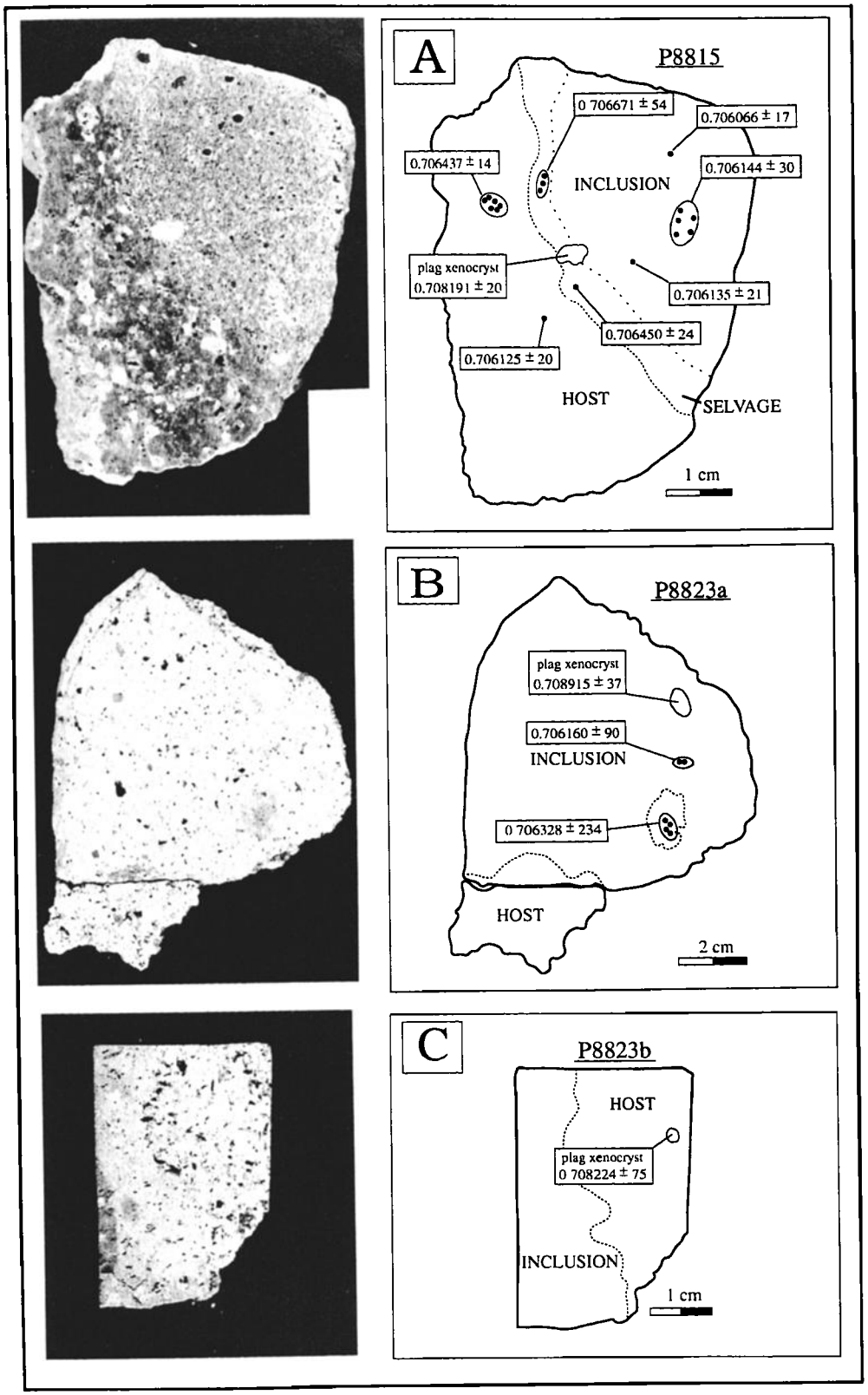

Fig. 6. (*a*) Microdrill sites and $^{87}Sr/^{86}Sr$ results from recovered material on sample P8815. The single hole drill site in the host actually sampled a tiny chilled fragment of mafic inclusion disseminated in the host (this is visable on high resolution large photographs of the slab), and thus gives a low $^{87}Sr/^{86}Sr$, relative to the multiple drill site (upper left) and the chips of the host. Photograph taken prior to cutting chips (cf. Figure 2). (*b*) and (*c*) Microdrill sites and results for two slabs from sample P8823. Note the high $^{87}Sr/^{86}Sr$ for the large plagioclase crystals in both inclusion (Figure 6*b*) and host (Figure 6*c*), indicative of a xenocrystic origin.

accordingly now most appropriately described as xenocrysts. The interface of the inclusion also has generally higher $^{87}Sr/^{86}Sr$ than the "bulk" host dacite. The interface appears to have a $^{87}Sr/^{86}Sr$ ratio of about 0.7067 (chip E on the host side of margin gives $^{87}Sr/^{86}Sr$ = 0.706735 ± 13: microdrill sites on the inclusion side of the margin shown in Figure 6*a* are $^{87}Sr/^{86}Sr$ = 0.706671 ± 54 and 0.706450 ± 24), while the host dacite is characterized by a $^{87}Sr/^{86}Sr \approx$ 0.7064 (chip G, furthest into the host dacite from the interface gives $^{87}Sr/^{86}Sr$ = 0.706432 ± 15, consistent with the multi-site microdrill result of $^{87}Sr/^{86}Sr$ = 0.706437 ± 14 shown in Figure 6*a*), so binary mixing between the inclusion and the dacite host cannot explain the isotopic or concentration data at the inclusion-host interface. The high Sr ppm and $^{87}Sr/^{86}Sr$ ratios observed in chip E might be due to incorporation of a larger amount of xenocrystic plagioclase; however, this is not consistent with the observation that this slice also has the highest Nd concentration and the lowest $^{143}Nd/^{144}Nd$ ratio (plagioclase typically contains very little Nd, and would not control the Nd isotopic composition of the sample).

5. Discussion

Our observations indicate that inclusion P8815 resulted from the mingling of a mafic magma with a silicic magma. However, the microsampling techniques used here have unraveled a set of characteristics of host and inclusion P8815 which require a complex interaction to account for them. For instance, the fact that the highest $^{87}Sr/^{86}Sr$ and lowest $^{143}Nd/^{144}Nd$ ratios are observed at the margin cannot be reconciled with the simple injection of mafic magma into an existing dacitic chamber. Further, if the marginal zone of the inclusion (either side of the weak chill defined by the selvage to the inclusion indicated on Figure 6*a* and a few millimeters into the host, represented by chip E in Figure 2) formed during interaction of the mafic and silicic magma and its isotopic composition reflects mixing between these two isotopically distinct reservoirs, then a third, now completely irradicated silica-rich, high $^{87}Sr/^{86}Sr$, endmember has to be postulated. The involvement of this third component is also supported by the "hybrid" character of the host dacite [cf. *Kouchi and Sunagawa*, 1985], as evidenced by its mixed crystal population and the presence of fragments with $^{87}Sr/^{86}Sr$ indistinguishable from the bulk inclusion within it (Figures 5 and 6).

The only clues as to the possible composition of the precursor silicic endmember come from (1) the cores of both the large plagioclase xenocrysts in the inclusion and those of R-type plagioclases in the host and (2) the core composition of the hornblende xenocryst. The $^{87}Sr/^{86}Sr$ ratios of the plagioclase cores (~0.709) arguably reflect the composition of the silicic endmember. This $^{87}Sr/^{86}Sr$ ratio is typical of the 4.2 Ma to ~1 Ma dacitic ignimbrites ($^{87}Sr/^{86}Sr$ = 0.708 - 0.711) which form the basement to Cerro Chascon [*de Silva*, 1989*b*]. Furthermore, the compositions of the xenocrystic plagioclase and hornblende cores (Table 1) are also typical of those in the ignimbrites (Figures 4*a* and 4*c*). We therefore suggest that a reasonable candidate for the silicic end member is a typical ignimbrite (or subvolcanic plutonic equivalents) from this region (Figure 7). This could either be residual magma left over from an ignimbrite eruption or a melt of pre-existing ignimbrite. For two main reasons we prefer the latter scenario; first, we consider it unlikely that residual magma from the last ignimbrite eruption (~1 Ma) would have survived until the Holocene (but see data of *Halliday et al.* [1989] for the still active 2.1 Ma Long Valley system). Second, to produce the characteristics of the "hybrid" host and the marginal zone, the mafic magma had to interact with a high-silica melt enriched in incompatible elements (i.e., Nd). The most likely composition for a residual ignimbrite magma in this region would be a dacite with SiO_2 ~64 - 68%, which is too low for the silica-rich endmember required to produce a mixed hybrid with up to 70% SiO_2 (see SiO_2 data of *Hawkesworth et al.* [1982]), but more important, such a magma would not have the enrichment in Nd that is required. However, a partial melt of such an ignimbrite, would not only have a eutectic composition, but also would be enriched in incompatible elements such as Nd, and therefore would be a more suitable endmember.

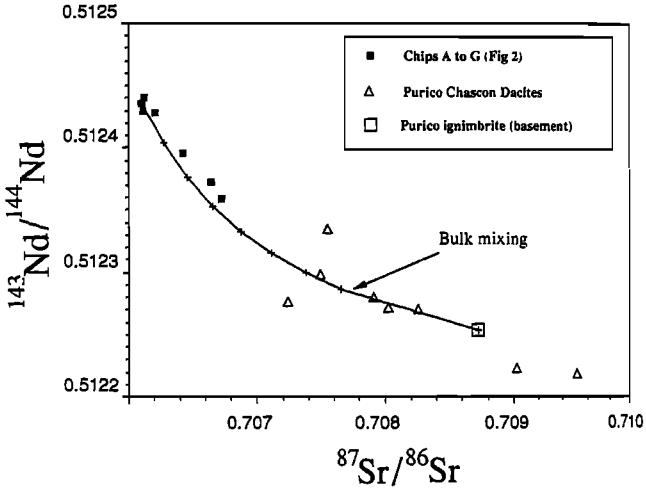

Fig. 7. $^{143}Nd/^{144}Nd$ - $^{87}Sr/^{86}Sr$ isotope diagram summarizing results of traverse in comparison with bulk analyses of Purico-Chascon dacites published by *Hawkesworth et al.* [1982], and the Purico ignimbrite [*de Silva*, 1987]. A calculated mixing curve between the basaltic andesite of the inclusion and the Purico ignimbrite is shown, suggesting that the isotopic data can be explained by mixing of the mafic liquid into the rhyodacite, with the maximum amount of contamination being preserved in the marginal zone (chip E). The mafic and silicic magmas were subsequently mixed to generate the host dacite. Crosses on the mixing curve are for increments of 10% ignimbrite mixed with the inclusion composition (80% and 90% not indicated).

Fig. 8. Schematic model for generating the observed relationships in sample P8815. (*a*) Stage 1: Mafic magma invades the ignimbrite beneath the Purico-Chascon complex, partially melting it to form a cap of rhyolitic magma with "felsic restite" (particularly plagioclase) characterized by the isotopic composition (high $^{87}Sr/^{86}Sr$) of the ignimbrite. (*b*) Stage 2: Further inputs of mafic magma result in convection in the rhyolite and breakdown of the mafic/silicic magma interface as mafic blobs are entrained into the rhyolite through viscous coupling at the interface. Exchange of crystal phases occurs, producing phases which are no longer in equilibrium (chemical, isotopic, or textural) with the local host, i.e., xenocrysts. The inclusions chill with a contaminated margin representing a mixture between the rhyolite and inclusion magma. The inclusion-forming magma is chemically modified to the basaltic andesite composition that we now observe. (*c*) Stage 3; More thorough mixing between the mafic and silicic magmas occurs, as the ratio of mafic to silcic magma increases and density stratification completely breaks down, to form a hybrid dacite (now seen as the host). Inclusions formed in stage 2 are chilled and not significantly affected, although further cooling and crystallization occurs in both host and inclusions.

A

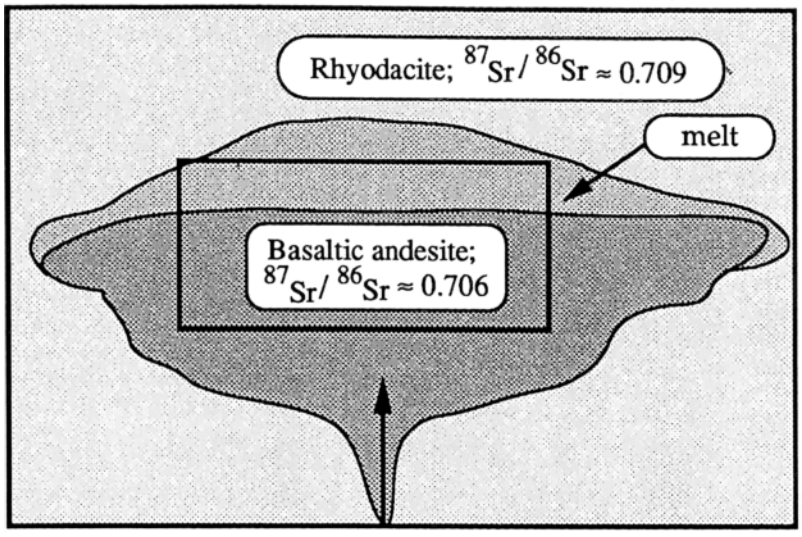

Mafic magma invades basement and melts pre-existing crust

B

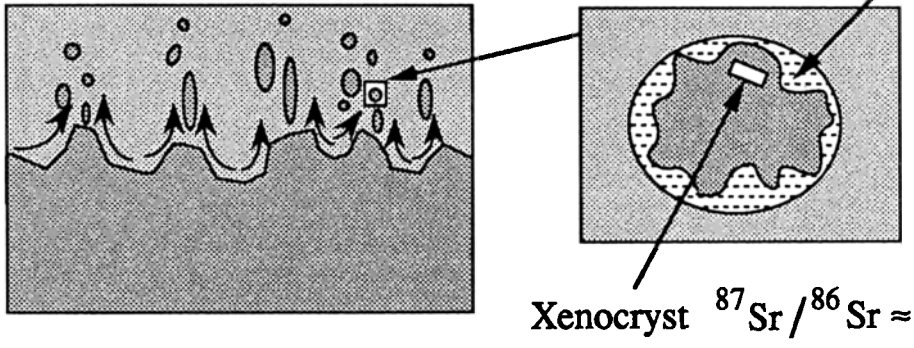

Pillows of mafic magma are entrained in silicic melt, with exchange of crystals and contamination of inclusion margins

C

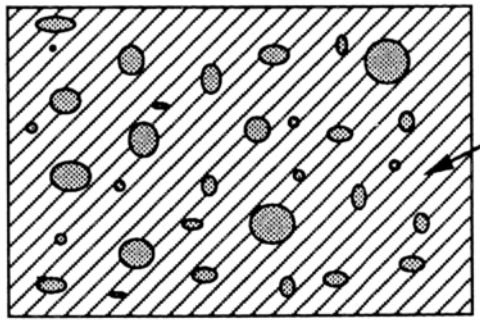

Mixing of mafic magma and silicic melt produces dacite hybrid - the host in which the inclusions are now found

During the mingling and mixing event, crystals from both the mafic and silicic systems were exchanged, giving rise to common "xenocrysts" within the host and occasional examples in the inclusion. Thermal equilibration was likely to have been rapid [*Sparks and Marshall*, 1986; *Frost and Mahood*, 1987], resulting in moderate degrees of undercooling. Precipitation of overgrowth rims in equilibrium with the new melt environment in each system, crystallization of the "hybrid" dacite host, and formation of plagioclase microlites ($An_{>60}$) within the inclusion would have occurred at this stage. The groundmass of the host represents the last phase of crystallization probably under conditions of accelerated cooling and decompression during eruption and emplacement. Finally, the similar glass compositions in host and inclusion indicate that thermal, but not neccesarily chemical, equilibration between the two phases had been reached: these are residual glass compositions and are the end result of crystallization from the respective systems. Our observations are similar to those from other "mixed" systems such as Chaos Crags [*Heiken and Eichelberger*, 1980] where abundant evidence for disequilbrium is found in the cores of large crystals. In these systems, similar glass compositions and different rim and microlite compositions in host and inclusion are believed to indicate thermal, but not chemical, equilibrium.

6. Petrogenetic Model

The presence of mafic inclusions argues for the interaction of a mafic magma with a more silicic one, and the juxtaposition of crystals derived from the two reservoirs within a hybrid dacite requires that the mixing event was vigorous. Further, the formation of a "hybrid" requires that a significant volume ratio of mafic magma would have to have interacted with the silicic magma [*Sparks and Marshall*, 1986; *Frost and Mahood*, 1987]. Our crude bulk mixing model (Figure 7) suggests that between 40 and 20% mafic magma (represented by the inclusions) was mixed into the silicic melt to produce the hybrid host (the Purico-Chascon dacites shown in Figure 7). These estimates are maxima, as the original mafic magma may have had higher $^{143}Nd/^{144}Nd$ and lower $^{87}Sr/^{86}Sr$ than the basaltic andesite inclusion now preserved. End-member dynamic models may be envisaged as either the direct injection of the mafic magma into an existing felsic magma reservoir or the overturn of a density and compositionally stratified chamber. Both mechanisms would be expected to yield a hybrid host on a local scale. However, at this stage we lean towards the latter scenario, as a two stage process where the silicic endmember is first produced by partial melting of ignimbrite and then interacts with the mafic magma is prefered. Figure 8 shows a schematic model for the origin of the host and inclusions. The details are neccesarily speculative, but the model can be regarded as a good working hypothesis constrained by the mineralogical and isotopic data.

Stage 1 (Figure 8*a*). Mafic magma, likely somewhat more magnesian than the present inclusion compositions, invades ignimbrite in the sub-Purico complex crust. The mafic magma ponds and cools, crystallizing olivine, augite, and plagioclase ($An_{>60}$). Partial melting of the ignimbrite results, producing a melt with a eutectic composition with enriched incompatible elements and with the same isotopic composition as the ignimbrite. Some of the phenocrysts from the ignimbrite will remain unmelted (i.e., large high $^{87}Sr/^{86}Sr$ plagioclases, low Mg# hornblendes and possibly biotite and quartz) and will provide a record for the involvement of the ignimbrite component. These may be termed "restite" in the manner of *Wyborn and Chappell* [1986], although "felsic restite" may be more appropriate.

Stage 2 (Figure 8*b*). As further inputs of mafic magma occur, the interface breaks down as small blobs of the mafic magma are entrained into the rhyolite due to convection and viscous coupling at the interface. Xenocryst exchange occurs during this process. The marginal zone of the inclusion mingles and mixes with the high $^{87}Sr/^{86}Sr$ and incompatible element enriched melt at small length scales, resulting in a hybrid margin compostion. The texture of the groundmass within this marginal zone (i.e., few skeletal crystals but large numbers of small crystals (Figure 3*d*)) suggests that the temperature difference between upper rhyolite and the mafic magma was not large, enhancing the likelihood of more intimate mixing as the ratio of mafic to silicic magma increased [e.g., *Sparks and Marshall*, 1986].

Stage 3 (Figure 8*c*). Overturn of the magma chamber causes intimate mixing of mafic magma (basaltic andesite inclusion precursor) with the rhyolite [cf. *Sparks and Marshall*, 1986], to produce the hybrid host dacite with inclusions of basaltic andesite. Limited exchange during pillowing/chilling and physical exchange of material (crystals) between host and inclusions produces the basaltic andesite inclusion composition from an initially more mafic magma, as discussed by *Sparks and Marshall* [1986]. The dacite contains both "xenocrysts" from the basaltic andesite and "felsic restite" (large high $^{87}Sr/^{86}Sr$ plagioclase, and Mg poor hornblendes) from the ignimbrite precursor. The microlite compositions suggest that they crystallized within their respective sub-systems late in the crystallization sequence, during which time resorption of xenocrysts and the subsequent overgrowth would have occurred. The tiny fragments of inclusion identified in the dacite may have resulted from disruption of larger inclusions due to vesiculation. Unlike at Lassen Peak [e.g., *Clynne*, 1989], wholesale disruption of inclusions after microlite formation is not indicated. Emplacement of the domes may have followed closely after the mixing event due to an increase in fluid pressure.

7. Implications

One of the main contributions of this work is to demonstrate the value of fine-scale determinations of trace element and isotope characteristics in geological materials, an area which the new generation of high-resolution ion probes should open up to the geosciences community in the next few years. This type of micro-sampling, in conjunction with more conventional detailed petrographic and microprobe work, allows a greater resolution of magmatic processes. Although we interpret the results from this initial study with caution, we believe that this type of data is a very neccesary adjunct to broader studies in constraining models of magmatic processes and may provide the fine tuning to already established models. Further measurements of this type on other inclusion-host pairs are in progress and will help increase our understanding of mafic-felsic magma interactions.

Acknowledgments. J.P.D and S.d.S thank Tim Druitt, Gerhard Wörner, Mike Clynne, and Charlie Bacon for fruitful and instructive discussions during the IAVCEI congress in Santa Fe, and Peter Francis for loan of his Land Rover and encouragement to take on the Purico project. The Turner Foundation of the University of Michigan (J.P.D) and the Royal Society of London (S.d.S) supported the fieldwork. Isotopic analysis at the University of Michigan was supported by NSF grant EAR 8720564. Charlie DeWolf is thanked for providing Pb isotope analyses. We thank Tom Vogel, John Reid, and Gerhard Wörner (official) and John Wolff and Ben Schuraytz (unofficial) for thoughtful and

helpful reviews of the manuscript. S.d.S is a visiting post-doctoral fellow at the Lunar and Planetary Institute, Houston, supported by NASA grant NAGW-1167, and would like to thank Vincent Yang at the Johnson Space Center for his help and advice with microprobe work. This is Lunar and Planetary Institute contribution number 733, and a contribution to IGCP project 249 "Andean Magmatism and its Tectonic Setting".

REFERENCES

Bacon, C.R., Magmatic inclusions in silicic and intermediate volcanic rocks, *J. Geophys. Res., 91,* 6091-6112, 1986.

Bacon, C.R., and T.H. Druitt, Compostional evolution of the zoned calcalkaline magma chamber of Mount Mazama, Crater Lake, Oregon, *Contrib. Mineral. Petrol., 98,* 224-256, 1988.

Bacon, C.R., and J. Metz, Magmatic inclusions in rhyolites, contaminated basalts and compositional zonation beneath the Coso volcanic field, California, *Contrib. Mineral. Petrol., 85,* 346-365, 1984.

Clynne, M.A., Disaggregation of quenched magmatic inclusions contributes to chemical diversity in silicic lavas of Lassen Peak, California (abstract), IAVCEI General Assembly. *Bull. N. M. Bur. Mines Miner. Resour., 131,* 54, 1989.

de Silva, S.L., Explosive silicic volcanism in the Central Andes of N. Chile, Ph.D. dissertation, 409 pp., The Open University, Milton Keynes, U.K., 1987.

de Silva, S.L., The origin and significance of crystal-rich inclusions in pumices from two Chilean ignimbrites, *Geol. Mag., 126,* 159-175, 1989*a*.

de Silva, S.L., Geochronology and stratigraphy of the ignimbrites from the 21° 30'S to 23° 30'S portion of the Central Andes of northern Chile, *J. Volcanol. Geotherm. Res., 37,* 93-131, 1989*b*.

Eichelberger, J.C., Origin of andesite and dacite: evidence of mixing at Glass Mountain and other circum-Pacific volcanoes, *Geol. Soc. Am. Bull., 86,* 1381-1391, 1975.

Francis, P.W., and S.L. de Silva, Application of the Landsat Thematic Mapper to the identification of potentially active volcanoes in the Central Andes, *Remote Sens. Environ., 28,* 245-255, 1989.

Francis, P.W., W.F. McDonough, M. Hammill, L.J. O'Callaghan, and R.S. Thorpe, The Cerro Purico shield complex, North Chile, in *Andean Magmatism - Chemical and Isotopic Constraints,* edited by R.S. Harmon and B.A. Barreiro, pp. 106-123, Shiva, Orpington, U.K., 1984.

Frost, T.P., and G.A. Mahood, Field, chemical and physical constraints on mafic-felsic magma interaction in the Lamarck Granodiorite, Sierra Nevada, California, *Geol. Soc. Am. Bull., 99,* 272-291, 1987.

Grove, T.L., and J.M. Donnelly-Nolan, The evolution of young silicic lavas at Medicine Lake Volcano, California: implications for the origin of compositional gaps in calc-alkaline series lavas, *Contrib. Mineral. Petrol., 92,* 281-302, 1986.

Halliday, A.N., G.A. Mahood, P. Holden, J.M. Metz, T.J. Dempster, and J.P. Davidson, Evidence for long residence times of rhyolitic magma in the Long Valley magmatic system: The isotopic record in precaldara lavas of Glass Mountain, *Earth Planet. Sci. Lett., 94,* 274-290, 1989.

Hawkesworth, C.J., M. Hammill, A.R. Gledhill, P. van Calsteren, and G. Rogers, Isotope and trace element evidence for late-stage intracrustal melting in the High Andes, *Earth Planet. Sci. Lett., 51,* 297-308, 1982.

Heiken, G., and J.C. Eichelberger, Eruptions at Chaos Crags, Lassen Volcanic National Park, California, *J. Volcanol. Geotherm. Res., 7,* 443-481, 1980.

Holden, P., A.N. Halliday, and W.E. Stephens, Neodymium and strontium isotope content of microdiorite-enclaves points to mantle input in granitoid production, *Nature, 330,* 53-56, 1987.

Kouchi, A., and I. Sunagawa, A model for mixing basaltic and dactic magmas as deduced from experimental data, *Contrib. Mineral. Petrol., 89,* 17-23, 1985.

Koyaguchi, T., Evidence for two-stage mixing in magmatic inclusions and rhyolitic lava domes on Nijima Island, Japan, *J. Volcanol. Geotherm. Res., 29,* 71-98, 1986.

Lesher, C.E., Kinetics of Sr and Nd isotope and chemical exchange between basalt and fusion products of the continental crust (abstract), *Eos Trans. AGU, 69,* 1509, 1988.

Sparks, R.S.J., and L.A. Marshall, Thermal and mechanical constraints on mixing between mafic and silicic magmas, *J. Volcanol. Geotherm. Res., 29,* 99-124, 1986.

Tait, S.R., Samples from the crystallizing boundary layer of a zoned magma chamber, *Contrib. Mineral. Petrol., 100,* 470-483, 1988.

Walker, G.P.L., and R.R. Skelhorn, Some associations of acid and basic igneous rocks, *Earth Sci. Rev., 2,* 93-109, 1966.

Wyborn, D., and B.W. Chappell, The petrogenetic significance of chemically related plutonic and volcanic rock units, *Geol. Mag., 123,* 619-628, 1986.

J. P. Davidson and P. Holden Department of Earth and Space Sciences, University of California, Los Angeles, CA 90024.

S. L. de Silva, Lunar and Planetary Institute, 3305 NASA Road 1, Houston, TX 77058.

A. N. Halliday, Department of Geological Sciences, University of Michigan, Ann Arbor, MI 48109.

(Received August 11, 1989;
revised January 30, 1990;
Accepted February 2, 1990.)